*inorganics*

MDPI

*Review*

# Affinity-Based Luminescent Iridium(III) Complexes for the Detection of Disease-Related Proteins

**Wanhe Wang [1,2,*,†], Jianhua Liu [1,2,†], Sang-Cuo Nao [3], Dik-Lung Ma [4], Jing Wang [1,2,*] and Chung-Hang Leung [3,*]**

[1] Institute of Medical Research, Northwestern Polytechnical University, 127 West Youyi Road, Xi'an 710072, China
[2] Chongqing Technology Innovation Center, Northwestern Polytechnical University, Chongqing 400000, China
[3] State Key Laboratory of Quality Research in Chinese Medicine, Institute of Chinese Medical Sciences, University of Macau, Macau SAR 999078, China
[4] Department of Chemistry, Hong Kong Baptist University, Hong Kong SAR 999077, China
* Correspondence: whwang0206@nwpu.edu.cn (W.W.); jwang0321@nwpu.edu.cn (J.W.); duncanleung@um.edu.mo (C.-H.L.)
† These authors contributed equally to this work.

**Abstract:** The occurrence of diseases is usually accompanied by changes in protein levels and types. These differentially expressed proteins can be used as biomarkers for the diagnosis and treatment of diseases. In recent years, luminescent iridium(III) complexes have attracted much attention in the field of protein-based disease diagnosis due to their excellent optical properties. In particular, affinity-based luminescent iridium(III) complexes have the advantage of evaluating protein information with minimal interference on their biological activities. In this review, we summarize the current advances in affinity-based luminescent iridium(III) complexes for the detection of disease-related proteins. Moreover, the future perspective for affinity-based iridium(III) complexes is discussed.

**Keywords:** affinity-based probe; iridium(III) complexes; luminescence; protein biomarkers; cancer; diagnosis



**Citation:** Wang, W.; Liu, J.; Nao, S.-C.; Ma, D.-L.; Wang, J.; Leung, C.-H. Affinity-Based Luminescent Iridium(III) Complexes for the Detection of Disease-Related Proteins. *Inorganics* **2022**, *10*, 178. https://doi.org/10.3390/inorganics10110178

Academic Editor: Peter Faller

Received: 24 September 2022
Accepted: 20 October 2022
Published: 25 October 2022



## 1. Introduction

A protein is a type of biological organic macromolecule composed of amino acids, and they are an important component of human cells and tissues [1]. Proteins account for about 18% of the total mass of the human body [2]. Dysregulations of protein (including changes in form, type, and abundance) are associated with a variety of diseases such as cancer, obesity, inflammatory disease, and metabolic disease. Therefore, proteins are valuable biomarkers for disease diagnosis [3,4].

Iridium(III) complexes are an emerging alternative luminescence modality to organic dyes, and have the characteristics of kinetic inertness, strong absorption in the ultraviolet region, high photoluminescence yield, large Stokes shift, photobleaching resistance, and environmentally sensitive luminescence [5–11]. In addition, the two-photon absorption capacity of iridium(III) complexes provides a near-infrared (NIR) window for improved tissue radiation penetration in biological imaging applications [12,13]. Furthermore, the relatively long phosphorescent lifetime of iridium(III) complexes provides an opportunity to use time-resolved luminescence techniques in order to significantly improve through the elimination of fluorescence background noise [14,15]. Functionalized with specific recognition elements, iridium(III) complexes have been widely applied for the detection of metal ions, small molecules, proteins, enzymes, and even cancer cells [16–24].

Generally speaking, luminescent probes for proteins are divided into activity-based probes (ABPs) and affinity-based probes (AfBPs) (Figure 1) [25,26]. Activity-based probes were originally established for proteome-wide profiling of kinases with covalent inhibitors

under native cellular settings. The design of activity-based probes is generally based on the incorporation of a reactive warhead into a high-affinity ligand. Commonly used reactive warheads include aryl sulfonyl fluoride, vinyl group, haloacetamide, and photoactivatable groups, which are capable of covalently binding to many nucleophilic amino acid residues, such as cysteine, tyrosine, threonine, lysine, and serine [27,28]. Covalent linking between the warhead and the target protein occurs, allowing analysis by mass spectrometry, fluorescence and/or radioisotope-assisted gel electrophoresis. This strategy is a powerful tool for the large-scale identification of potential "on" and "off" cellular targets of drug candidates. However, a disadvantage of activity-based probes is that by covalently binding to specific sites on proteins, such as enzyme active sites, they may interfere with the native biological activities of the proteins [29,30]. In contrast, affinity-based probes interact reversibly using non-covalent interactions including hydrogen bonding, electrostatic forces, van der Waals force, and hydrophobic interactions [31,32]. As affinity-based probes do not interact covalently with the target protein, they may have less effect on the native biological activities of the protein.

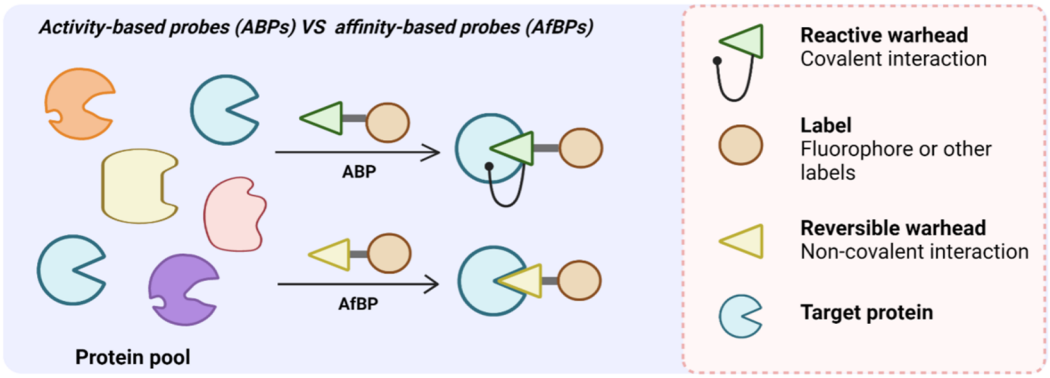


**Figure 1.** Schematic diagram of activity-based probes and affinity-based probes binding to the target protein.

Given the advantages of affinity-based probes, affinity-based luminescent iridium(III) complexes have been widely used in biomedical fields [3,33,34]. However, a comprehensive review on this topic is lacking. In this review, we summarize and discuss recent advances in the development and application of affinity-based iridium(III) complexes for various diseases, including cancer, inflammation, and other conditions (Figure 2). Moreover, the future directions for affinity-based iridium(III) complexes will also be discussed.

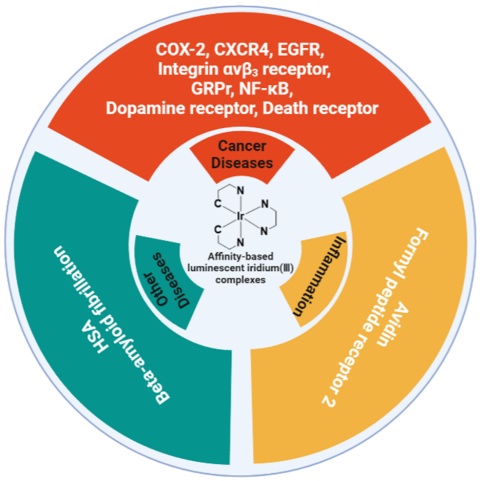


**Figure 2.** Affinity-based luminescent iridium(III) complexes for the detection of different disease-associated proteins.

## 2. Cancer-Related Probes

Cancer is a global public health problem [35]. In the past thirty years, the incidence rate of cancer in the world has increased by 3−5% per year, and cancer became the leading cause of death in 2020 [36]. The early diagnosis of cancer is particularly important to minimize cancer mortality [37,38]. Therefore, efforts have been made to develop optical imaging agents and inhibitors for the diagnosis and image-guided surgery of cancers. In this context, iridium(III) complex-based affinity-based probes have been explored for the detection and imaging of cancer-related proteins. Initially, the Lo group conducted landmark work of designing luminescent iridium–estradiol conjugates for the detection of breast cancer-related estrogen receptor α in a buffer [39]. After that, a range of affinity-based luminescent iridium(III) complexes were reported for the detection of cancer protein biomarkers.

### *2.1. COX-2-Specific Imaging Agents* (**1**−**2**)

Metabolism dysregulation is one of the hallmarks of cancer cells. Tumor cells often overexpress metabolic-related enzymes, and thus these enzymes are promising biomarkers for cancer detection [40,41]. In particular, COX-2 is a highly expressed enzyme in gastric cancer, colon cancer, pancreatic cancer, and other cancers, while it has very low expression in normal cells [42–44]. Ma and coworkers reported two new luminescent iridium(III) complexes **1** and **2** and evaluated their ability to detect COX-2 in human cancer cells [45]. These complexes represented the first application of iridium(III) complexes as COX-2 imaging agents. Complexes **1** and **2** possess a "binding unit" moiety that is a structural analogue of indomethacin, a COX-2 inhibitor, that is linked to the iridium(III) "signal unit" via an amide bond. This modular design can yield suitable probes that retain specific binding to the target enzyme for detection. Complex **1** shows a maximum emission wavelength at 575 nm, while complex **2** exhibits a maximum emission at 580 nm, with large Stokes shifts of around 280 nm for both complexes. Complexes **1** and **2** showed strong and stable luminescence in HeLa cells expressing high levels of COX-2, while they displayed negligible luminescence in LO2 cells that express low levels of COX-2 (Figure 3B,C). These results indicate that complexes **1** and **2** could be used to distinguish cancer cells from normal cells based on their COX-2 expression status. A drawback of these complexes is that they are "always-on" COX-2 probes with low imaging contrast.

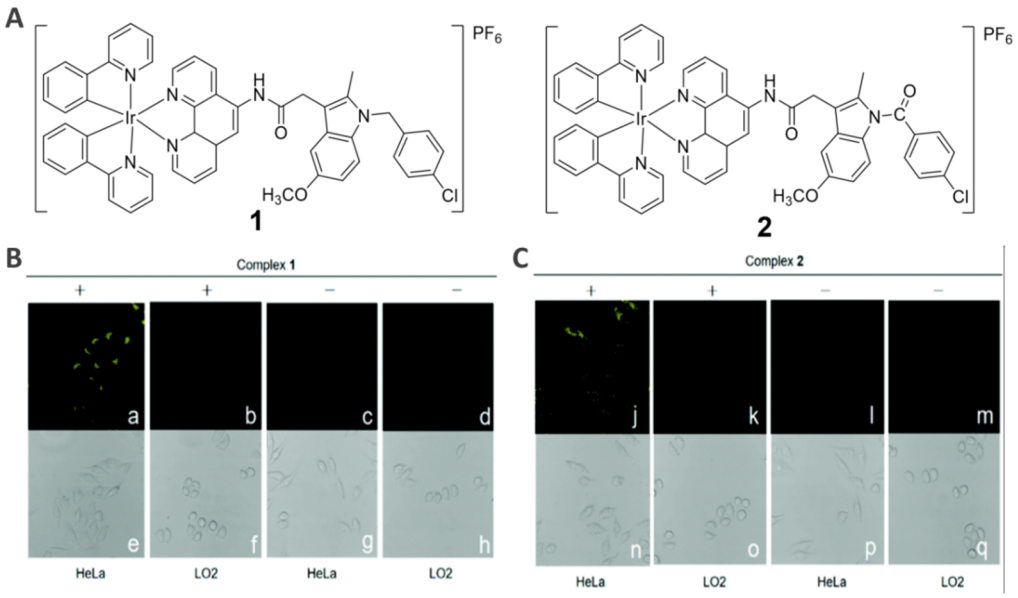


**Figure 3.** (**A**) Chemical structures of complexes **1**−**2**. Living cells stained by (**B**) complex **1** and (**C**) complex **2** (1.0 μM). (a, c, e, g, j, l, n, p) HeLa cells and (b, d, f, h, k, m, o, q) LO2 cells. The upper row is luminescence imaging, and the lower row is bright field imaging. $\lambda_{exc}$ = 405 nm. Reproduced with permission from ref. [45]. Copyright 2017 Royal Society of Chemistry.

### *2.2. Integrin αvβ3 Receptor-Specific Imaging Agents* (**3**)

As a targeting motif, RGD mediates specific binding with the $\alpha_v\beta_3$ integrin receptor, which is highly expressed in various tumor tissues, so RGD-derived molecules have been widely applied for optical imaging and drug delivery systems [46]. Ma et al. reported an iridium(III)–histidine coordination (Ir−HH cyclization)-based method for cyclization and preparation of an RGD-cyclized iridium(III) complex (Ir−HRGDH, **3**) (Figure 4A) [47]. The process of the cyclization reaction can be readily monitored by the increase in the phosphorescence intensity of the resulting complex formed. Complex **3** shows a maximum emission wavelength at 492 nm under excitation at 328 nm. Moreover, complex **3** showed extensive phosphorescence distribution in the cytoplasm of the $\alpha_v\beta_3$ integrin-overexpressing cancer cell line A549, while a linear RGD-labeled iridium(III) complex (RGDHH−Ir) only showed weak phosphorescence staining, which is attributed to the stronger membrane permeability of cyclic peptides. Furthermore, compared with the conventional fluorescein-labeled cyclic RGDyK peptide, complex **3** showed better targeting affinity for cancer cells with stronger membrane permeability (Figure 4B). This work provides an efficient method to prepare cyclic peptide-functionalized metal complexes, which will largely improve their membrane permeability.

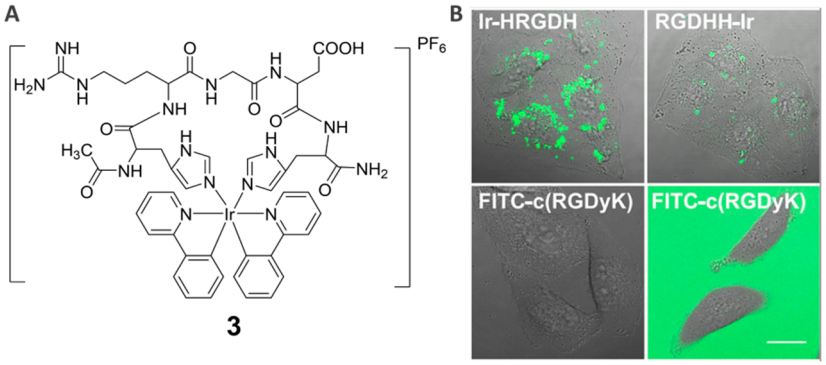


**Figure 4.** (**A**) Chemical structure of complex **3**. (**B**) Images of A549 cells incubated with Ir−HRGDH (10 μM, $\lambda_{exc}$ = 405 nm), RGDHH−Ir (10 μM, $\lambda_{exc}$ = 405 nm), or FITC−c(RGDyK) (10 μM, $\lambda_{exc}$ = 488 nm) for 24 h at 37 °C. Reproduced with permission from ref. [47]. Copyright 2014 American Chemical Society.

### *2.3. CXCR4-Specific Imaging Agents* (**4**−**6**)

Chemokine receptor 4 (CXCR4) is a G protein-coupled membrane receptor, which is overexpressed in 23 types of cancer and is highly associated with tumor metastasis [48–51]. Joeri et al. reported three different Ac-TZ14011 peptide-conjugated iridium(III) complexes (**4**−**6**) for imaging CXCR4-overexpressing breast cancer cells (Figure 5A) [52]. Ac-TZ14011 is a peptide with an affinity for CXCR4 [53]. Complexes **4**−**6** showed absorption maxima at 383, 397, and 410 nm and emission maxima at 585, 572, and 566 nm, respectively. Moreover, the lifetimes of the three complexes were all over 200 ns in a nondegassed solvent, which is much longer than the measured lifetime of 4.4 ns for the organic dye rhodamine 101. Complexes **4**−**6** bound to CXCR4 with $K_d$ values of 84.4 nM, 254.4 nM, and 66.3 nM, respectively. Cell-imaging experiments demonstrated that complexes **4**−**6** stained CXCR4-overexpressing MDA-MB-231 cells (Figure 5B), and their luminescence intensity was correlated with their $K_d$ values. Benefiting from the long emission lifetime of iridium(III) complexes, fluorescence lifetime imaging of complex **6** stained the cell membrane with a high signal-to-noise ratio. This work harnessed well the desirable photophysical properties of iridium(III) complexes for imaging cancer cells.

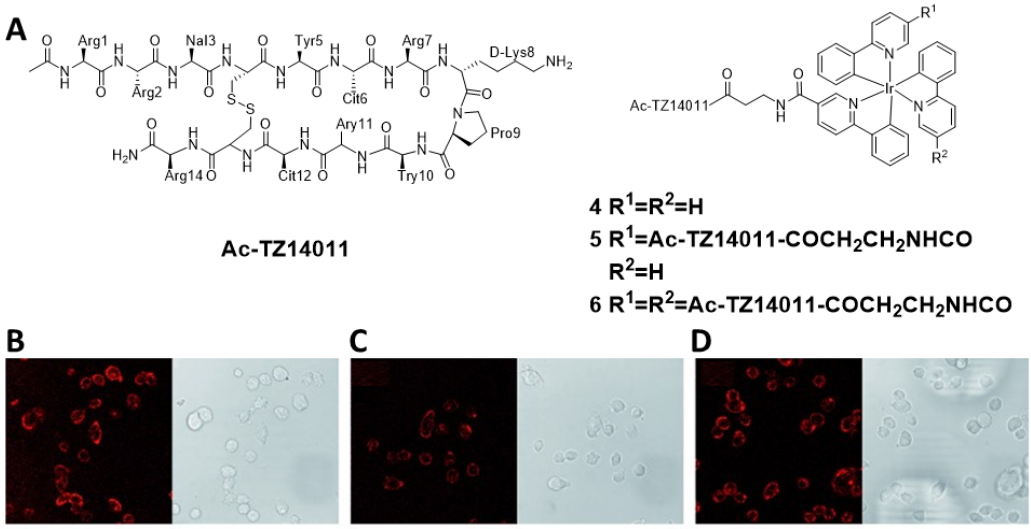


**Figure 5.** (**A**) Chemical structures of complexes **4**—**6**. Confocal images of the peptide-conjugated iridium(III) complexes in CXCR4-expressing MDA-MB-231 cells: (**B**) **4** (1 μM); (**C**) **5** (1 μM); (**D**) **6** (1 μM). Reproduced with permission from ref. [52]. Copyright 2011 John Wiley and Sons.

### *2.4. EGFR-Specific Theranostic Agents* (**7**)

Epidermal growth factor receptor (EGFR) is the receptor of epidermal growth factor (EGF), a regulator of signal transduction and cell proliferation [54,55]. EGFR overexpression is highly linked to tumor angiogenesis, cell proliferation, tumor invasion, and metastasis. In 2020, Wu et al. grafted a well-known EGFR inhibitor, 2-(4-hydroxybenzylidene)malononitrile [56], as a "binding unit" into iridium(III) complexes (signal units) for the generation of a series of EGFR probes (Figure 6) [57]. The maximum emission wavelength of these complexes is mainly located in the range of 529—611 nm. Among them, complex **7** showed characteristic absorbance bands of transition metal complexes at 208—346 nm, with a Stokes shift of over 200 nm (Figure 6A), which was much larger than the typical Stokes shifts of fluorescent dyes. Moreover, complex **7** showed bright luminescence in the EGFR-overexpressing human epidermoid carcinoma cell line A431. Target engagement of complex **7** was verified with a competition experiment using an EGFR inhibitor, as well as a colocalization experiment where the green–yellow color of complex **7** perfectly overlaid with green immunofluorescence in A431 cells with a Pearson's correlation coefficient of 0.950 (Figure 6B). Further inhibition experiments demonstrated that complex **7** suppressed EGFR activity with an $EC_{50}$ value of 1.18 μM, while it inhibited A431 cells through the EGFR-mediated MEK/ERK pathway in A431 cells. Thus, this work indicates the desirable theranostic potential of affinity-based iridium(III) complexes. However, the "always–on" luminescence mode of complex **7** requires washing steps for imaging, which is a drawback.

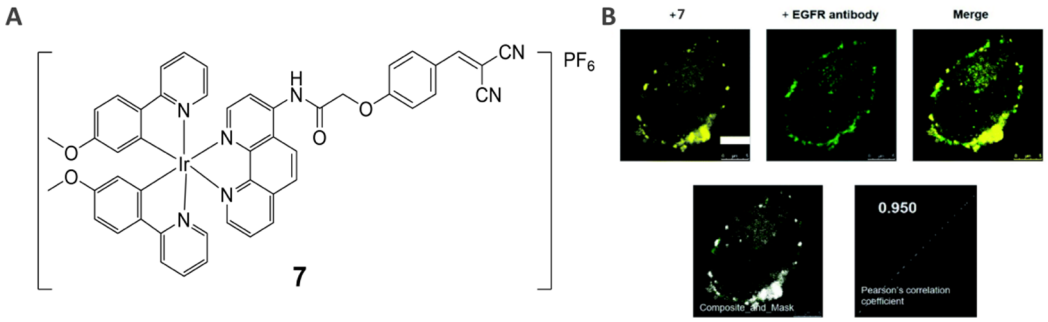


**Figure 6.** (**A**) Chemical structures of complex **7**. (**B**) Co-localization studies of complex **7** (1 μM, 30 min) with immunofluorescence imaging in A431 cells ($\lambda_{exc}/\lambda_{emi}$ = 405 nm/500—700 nm). Reproduced with permission from ref. [57]. Copyright 2020 American Chemical Society.

### *2.5. GRPr-Specific Theranostic Agents* (**8**)

Gastrin-releasing peptide receptor (GRPr) is a member of the bombesin G protein-coupled receptor family, and its aberrant expression is highly associated with a range of cancers including kidney, prostate, lung, and colorectal cancers [58–60]. Wang et al. reported an iridium(III) complex (**8**) functionalized with a GRPr peptide-based inhibitor, JMV594, for studying of GRPr functions in living cancer cells and immune cells (Figure 7A) [61]. In this work, a long alkyl 6-aminohexanoic acid was selected as a linker to conjugate an iridium(III) complex and JMV594, ensuring the retention of specific GRPr binding of JMV594 to the conjugate. Complex **8** exhibited an intense absorption band of spin-allowed intraligand ($^1$IL) at 250−310 nm and a less-intense absorption band of spin-allowed metal-to-ligand charge-transfer ($^1$MLCT) transition at 310−450 nm in acetonitrile (ACN), while it had an emission maxima at 596 nm, with a large Stokes shift of 275 nm. Imaging experiments showed that the complex was capable of imaging GRPr-positive lung cancer A549 cells, and its target engagement was verified by a knockdown experiment, where the yellow luminescence of complex **8** was only observed in cells not treated with GRPr siRNA (Figure 7B). Moreover, complex **8** also inhibited GRPr activity-related production of proinflammatory cytokines including TNF-$\alpha$ in LPS-induced RAW264.7 cells. The theranostic property of complex **8** makes it suitable for the deep understanding of GRPr functions in cancers, and its feasibility in in vivo use should be studied in the future.

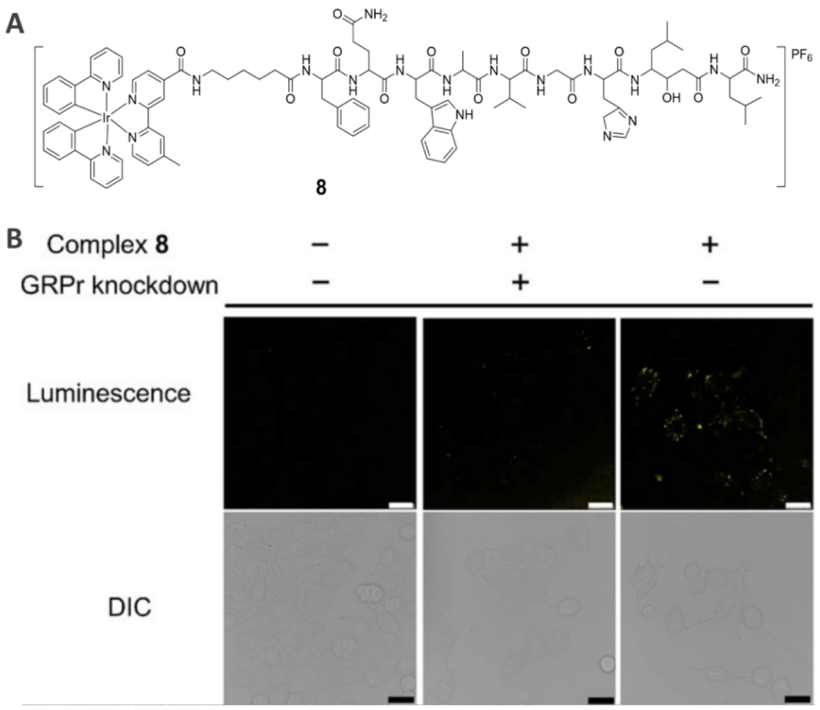


**Figure 7.** (**A**) Chemical structure of complex **8**. (**B**) Effect of GRPr knockdown on the imaging of A549 cells. A549 cells and GRPr knockdown A549 cells were incubated with or without complex **8** (10 μM) for 2 h. Cell images were detected at $\lambda_{exc}/\lambda_{emi}$ = 405/570−690 nm. Reproduced with permission from ref. [61]. Copyright 2020 John Wiley and Sons.

### *2.6. Dopamine Receptor-Specific Imaging Agents* (**9**−**12**)

Dopamine receptor is a kind of receptor located in the cell membrane, and its abnormal expression was recently identified to be linked with several types of cancers including lung cancer, breast cancer, and colon cancer [62–64]. Ma and coworkers reported a series of luminescent iridium(III) complexes (**9**−**12**) containing dopamine moieties as dopamine receptor (D1R/D2R) bioimaging probes (Figure 8A) [65]. These complexes were designed to specifically bind to the dopamine receptor based on the interaction between their dopamine moiety and dopamine receptor. Among them, complexes **9** and **11** showed long emission

lifetimes of 4.61 μs and 4.36 μs, respectively, while complex **11** had the most brightness with a quantum yield of 0.245, with emission centered at 558 nm and a large Stokes shift of 215 nm. Moreover, these two complexes showed low cytotoxicity (>100 μM) in A549 cells. Imaging experiments showed that complexes **9** and **11** selectively visualized A549 cells, and their yellow luminescence was largely reduced after dopamine receptor siRNA treatment (Figure 8B−D). The long lifetime of complex **11** was further exemplified by a fluorescence lifetime imaging experiment in which intracellular background fluorescence was largely eliminated. This work highlights the merits of using iridium(III) complexes for cell imaging.

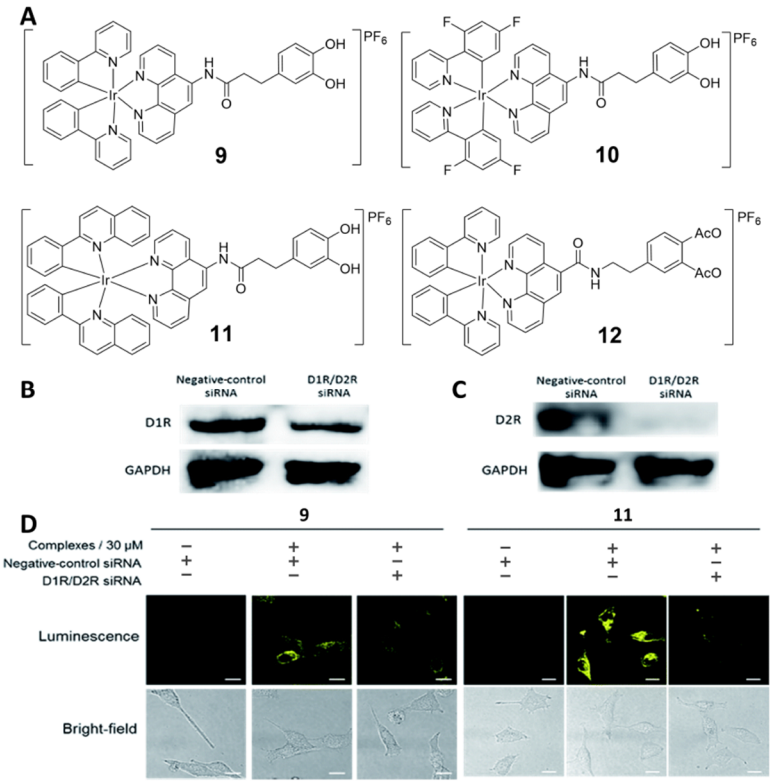


**Figure 8.** (**A**) Chemical structures of complexes **9**−**12**. The relative amount of D1R/D2R in A549 cells before (**B**) or after (**C**) D1R/D2R siRNA treatment. (**D**) Cell images of A549 cells with complexes **9** and **11** in D1R/D2R knockdown experiment. A549 cells were incubated with or without complexes **9** and **11** (30 μM) for 1 h. Reproduced with permission from ref. [65]. Copyright 2018 Royal Society of Chemistry.

### *2.7. Death Receptor-Specific Theranostic Probe* (**13**)

Apoptosis is an essential biological process for maintaining the balance of the internal environment [66,67]. However, abnormal apoptosis increases the risk of tumorigenesis, as abnormal cells fail to be removed from the body [68]. Tumor necrosis factor-related apoptosis-inducing ligand (TRAIL) can trigger the cell-exogenous apoptosis pathway by binding with death receptors (DR4 and DR5) and other related signaling receptors [69,70]. Aoki and coworkers reported a luminescent tris homoleptic iridium(III) complex-peptide hybrid **13**, which contains a DR5-specific cyclic peptide [71]. Complex **13** exhibited maximum absorption bands of about 280 and 360 nm, with a strong green emission peak at about 506 nm. Moreover, the complex had a luminescence quantum yield of 0.35 and an emission lifetime of 1.0 μs. Its specific binding to DR5 was determined to be $K_d$ of 2.2 μM by a 27 MHz quartz-crystal microbalance (QCM) measurement. Complex **13** induced apoptosis similar to TRAIL in Jurkat cells. Further imaging experiments validated that complex **13** selectively imaged Jurkat cells based on the high expression of DR5, which

was consistent with an immunofluorescence imaging experiment (Figure 9B). Complex **13** further highlights the theranostic application of iridium(III) complexes.

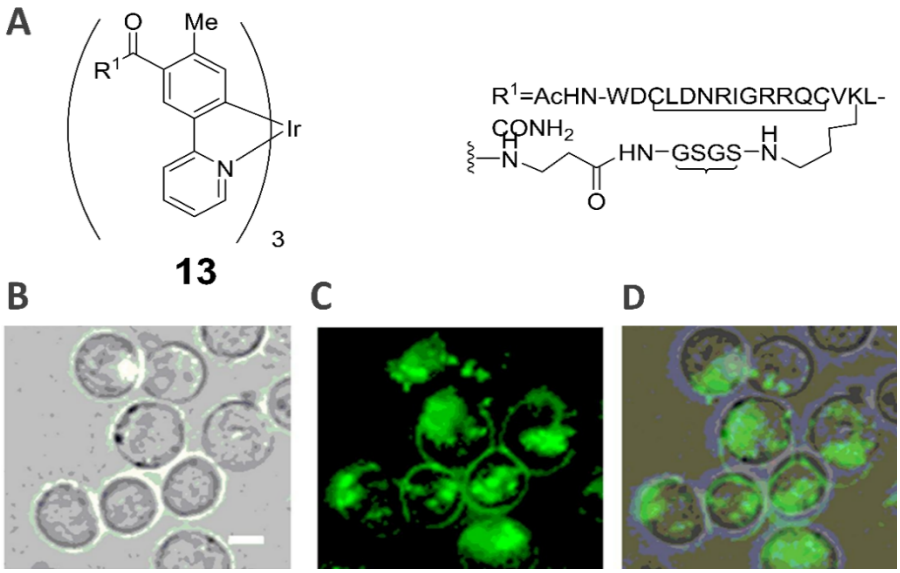


**Figure 9.** (**A**) Chemical structures of complex **13**. Luminescence images of Jurkat cells incubated with complex **13** (5 μM) at 37 °C for 1 h. (**B**) bright image, (**C**) emission image, (**D**) overlay image of (**B**,**C**). Scale bar (white) = 10 μm. Reproduced with permission from ref. [71]. Copyright 2018 Elsevier.

## 3. Inflammation-Related Probes

### *3.1. Avidin-Specific Luminescence Probes* (**14**−**15**)

Biotin is essential for the normal metabolism of fats and proteins, playing an important role in maintaining the natural growth and development of the human body [72]. The strong binding effect between biotin and avidin has been widely used for biomolecular detection, immunoassays, and clinical diagnosis [73]. Since 2004, a series of iridium–biotin conjugates were reported for "turn-on" detection of avidin in solution [74–79]. In 2008, Kwon et al. reported a tripod probe (**14**) for biotin–avidin assays, which consists of an energy acceptor (iridium(III) complex), an energy donor, and biotin, while a probe without donor (**15**) served as a control (Figure 10A) [80]. The luminescence of probes **14** and **15** originated from both $^1$MLCT (d$\pi$(Ir)→$\pi^*$(N-O)) and $^3$LC in the iridium(III) complex, and they also had similar emission maxima at around 472 nm in ACN, along with emission lifetimes of 0.49 μs and 0.45 μs, respectively. Upon binding to avidin, probes **14** showed a ca. 14-fold luminescence enhancement at a **14**/avidin ratio of 4:1 under excitation at an absorption peak of the donor (310 nm), due to enhanced intramolecular energy transfer and hydrophobicity after binding. This phenomenon was not observed in probe **15** due to the lack of enhanced intramolecular energy transfer. However, the feasibility of this probe for living systems was not explored.

### *3.2. Formyl Peptide Receptor-Specific Imaging Agent* (**16**)

Formyl peptide receptors (FPRs) play important roles in defense responses, neurodegenerative diseases, tumors, and metabolism-related disorders, and are emerging as potential therapeutic targets in wound repair and inflammatory diseases [81,82]. The Ma group developed a luminescent peptide WKYMVm-conjugated iridium(III) complex **16** as a luminescent FPR2 imaging probe in living cells (Figure 11A) [83]. WKYMVm is a highly selective FPR2 agonist [84]. Complex **16** had an emission maximum at 576 nm and an excitation maximum at 291 nm. Moreover, complex **16** also showed a good quantum yield of 0.245 along with a long emission lifetime of 4.62 μs. Cell-imaging experiments showed that complex **16** can selectively imaging FPR2-expressing HUVEC cells, but its luminescence was largely reduced in the presence of FPR2 siRNA (Figure 11B). Target

engagement results are also supported by a competitive analysis with a known FPR2 antagonist WRW4. Furthermore, complex **16** effectively reduced inhibited lipoxygen-A4 (LXA4)-induced HUVEC cell migration, demonstrating its theranostic ability for imaging and inhibiting FPR2 functions in living cells. This is the first report of employing long-lived iridium(III) probe for studying FPR2 functions in living systems.

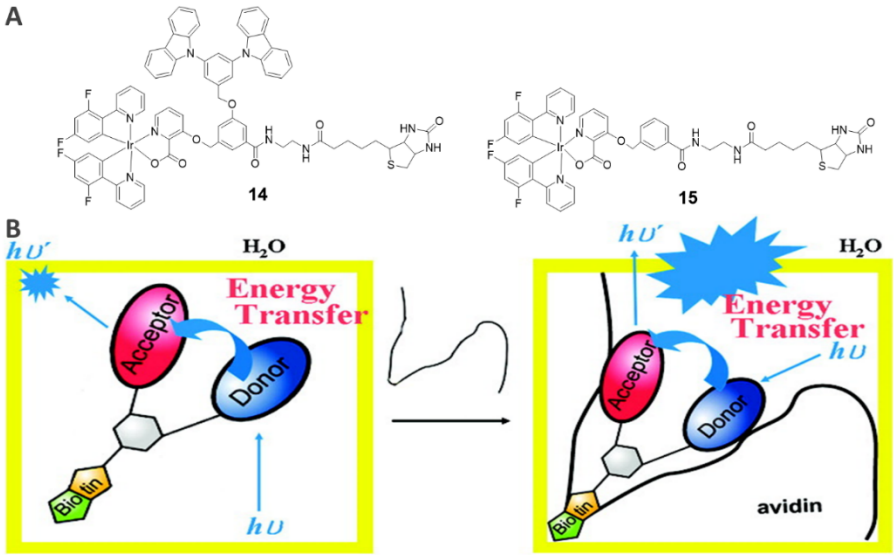


**Figure 10.** (**A**) Chemical structures of complexes **14**−**15**. (**B**) Schematic illustration of complex **14** to detect avidin. Reproduced with permission from ref. [80]. Copyright 2008 American Chemical Society.

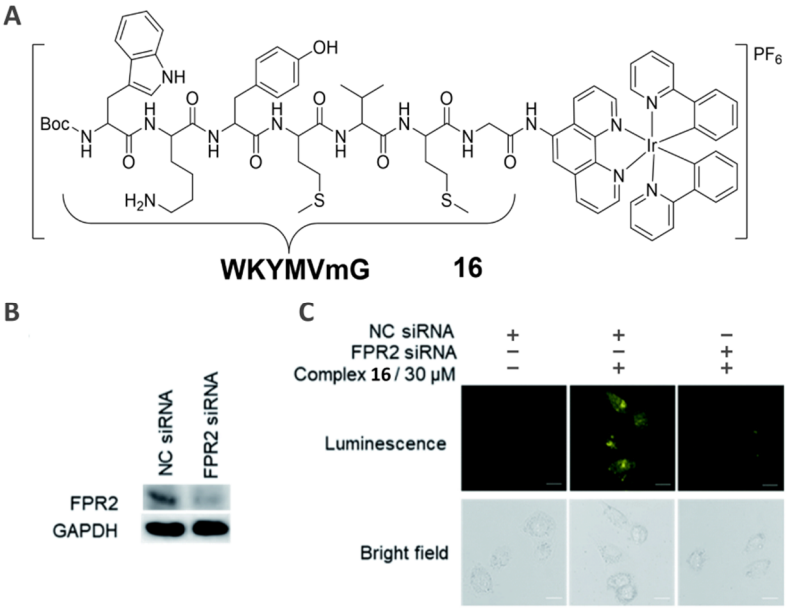


**Figure 11.** (**A**) Chemical structure of complex **16**. (**B**) FPR2 expression after the treatment of FPR2 siRNA. GAPDH was used as a loading control. (**C**) Normal HUVEC cells and FPR2 knockdown HUVEC cells were stained with or without complex **16** (30 μM) for 1 h. Reproduced with permission from ref. [83]. Copyright 2018 Royal Society of Chemistry.

### *3.3. NF-κB-Specific Imaging Agent* (**17**)

NF-κB is a critical transcription factor that plays an important role in mediating inflammation, immune responses, and cell proliferation [85,86]. The related bioimaging probes are desirable for unmasking its roles in immune systems. The Ma group developed a natural

product-conjugated iridium(III) complex **17** to track intracellular NF-κB (Figure 12A) [87]. Oridonin is a selective binder of the p50 subunit of NF-κB. Complex **17** showed a luminescence band centered at around 577 nm, with a Stokes shift of about 277 nm. Imaging experiments showed that complex **17** was capable of detecting NF-κB in HeLa cells, and this luminescence was decreased in cells pretreated with p50 siRNA (Figure 12B). Moreover, this probe can track tumor necrosis factor-α (TNF-α)-induced NF-κB translocation from the cytoplasm into the nucleus. A luciferase reporter assay confirmed its weak NF-κB inhibitory activity in HeLa cells. Complex **17** could potentially be applied as a theranostic probe for NF-κB, but its inhibitory activity requires improvement for therapeutic applications.

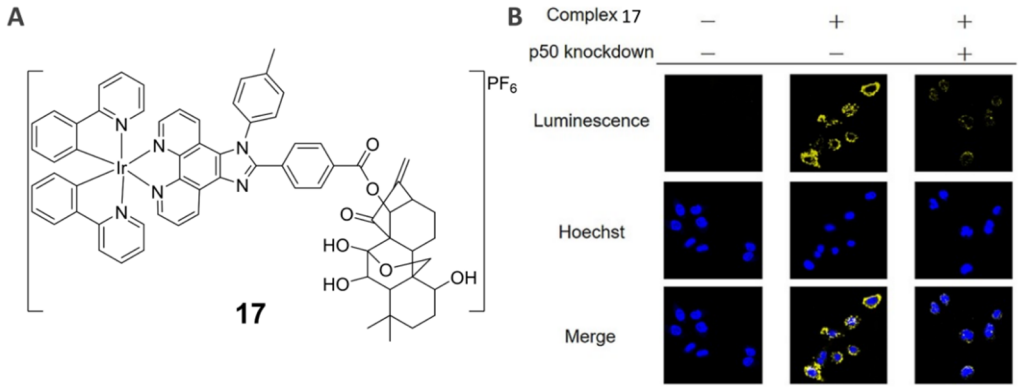


**Figure 12.** (**A**) Chemical structure of complex **17**. (**B**) Effects of p50 knockdown on the tracking of NF-κB in HeLa cells. Normal HeLa cells and p50 knockdown HeLa cells were treated with or without **17** (10 μM) for 4 h followed by stimulation with TNF-α (25 ng/mL) for 20 min. The yellow color indicates the luminescence from complex **17**, while the blue color indicates the fluorescence from Hoechst 33342 in the nucleus. Reproduced with permission from ref. [87]. Copyright 2017 John Wiley and Sons.

## 4. Other Disease-Related Protein Probes

### *4.1. Human Serum Albumin (HSA)-Specific Staining Probes* (**18**)

The level of human serum albumin (HSA) in the blood or urinary system is an important indicator of kidney disease, hypoalbuminemia, and microalbuminuria, so the detection of HSA is of great significance for clinical diagnosis and drug discovery [33,88]. In 2018, Wang et al. reported an iridium(III) complex **18** for the turn-on detection of HSA in the urinary system (Figure 13A) [89]. The emission lifetime and quantum yield of complex **18** in PBS solution were 52 ns and 0.002, respectively, and these values increased to 101 ns and 0.048, respectively, upon addition of HSA. The complex showed a maximal ca. 26.7-fold phosphorescence enhancement in PBS solution in response to HSA, with a detection limit of 0.8 $\mu g/mL^{-1}$ (Figure 13B). Moreover, complex **18** only showed minimal interference from other proteins including hemin, trypsin, lysozyme, apo-transferrin, catalase, bovine serum albumin, hemoglobin, methemoglobin, holo-transferrin, myoglobin, and transferrin (Figure 13C). Competition and molecular docking experiments suggested that complex **18** was a potential site I- and II-binding probe for HSA. The different luminescence response between HSA and BSA was attributed to its different binding mode, where complex **18** only bound to site II of BSA. Furthermore, the probe can selectively stain HSA in gel electrophoresis, and was much clearer than Coomassie blue. Interestingly, complex **18** has no specific binding unit for HSA, which is common among affinity-based probes.

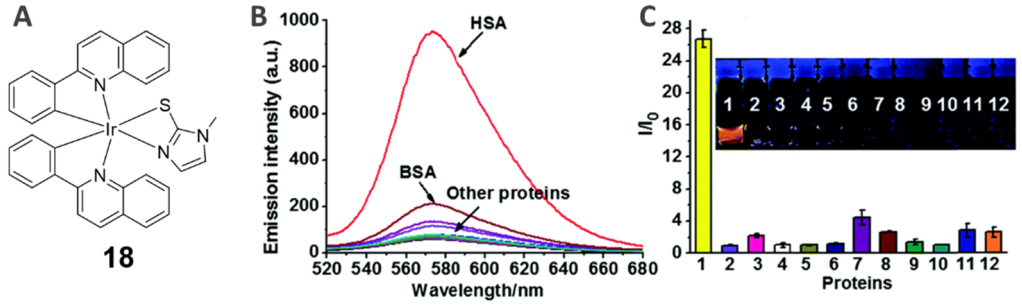


**Figure 13.** (**A**) Chemical structure for complex **18**. (**B**) The phosphorescence spectra of complex **18** (5 μM) in the presence of various proteins (50 μg $mL^{-1}$). (**C**) The turn-on phosphorescence ratio of complex **18** with different proteins. Reproduced with permission from ref. [89]. Copyright 2018 MDPI AG.

### *4.2. Beta-Amyloid Fibrillation-Specific Theranostic Probes* (**19**−**21**)

Aβ peptides are amphipathic peptides consisting of 39−42 amino acids (AAs), in which Aβ40 and Aβ42 are the major human Aβ peptides [90]. In particular, Aβ42 can rapidly form plaques and fibrils and is the main component of amyloid plaques or fibrils in the cerebrospinal fluid of Alzheimer's disease (AD) patients. Assembled plaques and fibrils are highly toxic to brain cells, ultimately resulting in AD [91]. Curcumin is a polyphenolic compound extracted from the rhizome of *Zingiberaceae* which was found to specifically interact with Aβ peptides based on an affinity mode [92,93]. Zhao et al. synthesized a series of iridium(III) complexes (**19**−**21**) with curcumin as the ancillary ligand (Figure 14) [34]. All complexes exhibited emission lifetimes of 1.29−1.79 μs, emission maxima of 520−600 nm, and Stokes shifts of over 200 nm. The complexes showed significant luminescence enhancement to Aβ42 fibers, and only a slight enhancement to Aβ42 monomers. The best complex **21** showed 50-fold and 470-fold luminescence enhancement to Aβ42 monomers and Aβ42 fibrils, respectively. Moreover, complex **21** exhibited the strongest inhibition of Aβ42 peptide aggregation, which was verified by ThT fluorescence assay and transmission electron microscope (TEM) imaging. Complex **21** displayed an inhibitory effect on the aggregation of Aβ42. However, its in cellulo luminescence imaging application was not explored.

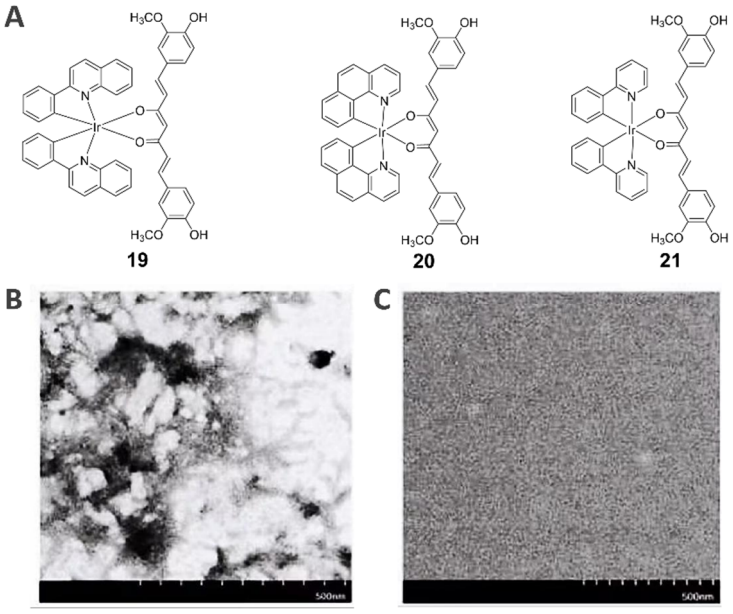


**Figure 14.** (**A**) Chemical structures for complexes **19**−**21.** Inhibition of seed-induced Aβ42 fibrillation by complex **21** shown by TEM images of Aβ42 fibrillation in the (**B**) absence or (**C**) presence of 50 μM of complex **21**. Reproduced with permission from ref. [34]. Copyright 2021 Elsevier.

## 5. Conclusions and Perspective

As a type of transition metal complex, iridium(III) complexes have many advantages beyond traditional organic probes, such as tunable emission from visible light to the NIR region, large Stokes shift, high stability, long emission lifetime, and potential applications in biosensors. In this review, affinity-based iridium(III) probes were mainly described. Compared with activity-based probes, they have broader applications and are also less likely to interfere with the native biological function of the protein target. In this review, we have described affinity-based iridium(III) probes for a range of protein targets, including tumor-related proteins, transcription factors, G protein-coupled receptors, dopamine receptors, and Aβ peptides.

With the advent of advanced techniques in imaging and drug development, the reported iridium(III) complexes have further research value in the fields of super-resolution microscopy, NIR-II imaging, photoacoustic imaging, biomedical applications, and even clinical use. Indeed, transition metal complexes have shown great potential as multifunctional anticancer compounds integrating imaging and therapeutic functions [94–96]. However, the research on affinity-based iridium(III) complexes is still in its infancy, and there are still many problems to be solved. Some of the affinity-based iridium(III) complexes are permanent luminescence probes, and they have no luminescence change upon binding with corresponding proteins. These probes suffer from low signal-to-noise, and usually require further washing steps in cell imaging. Another issue that has to be further explored for affinity-based iridium(III) probes is the linker region that is used to connect the iridium(III) complexes to the binding units. Currently, the precise effects of linkers on the luminescence behaviors and binding affinity of the probes are less understood. Furthermore, the exact mechanisms of cellular uptake, transport, storage, and metabolism of these compounds are not very clear, but are prerequisites for further clinical application. Finally, the cytotoxicity issues of iridium(III) complexes also need to be considered alongside their imaging and binding ability. We believe that more and more efforts from bioinorganic and other fields will accelerate and advance affinity-based iridium(III) complexes into disease diagnosis and therapy in the clinical setting.

**Author Contributions:** Conceptualization, W.W., J.W. and C.-H.L.; methodology, J.L.; data curation, W.W. and J.L.; writing—original draft preparation, W.W. and J.L.; writing—review and editing, W.W., S.-C.N., J.W. and C.-H.L.; supervision, W.W., D.-L.M., J.W. and C.-H.L.; project administration, W.W., J.W. and C.-H.L.; funding acquisition, W.W., J.W. and C.-H.L. All authors have read and agreed to the published version of the manuscript.

**Funding:** This research was funded by the Natural Science Basic Research Program of Shaanxi (2021JQ-089, 2021JQ-092), the Natural Science Foundation of Chongqing, China (cstc2021jcyj-msxmX0659), the National Natural Science Foundation of China (22101230), the Fundamental Research Funds for the Central Universities (31020200QD017, 31020200QD023), Shanghai Sailing Program (21YF1451200), the Guangdong Basic and Applied Basic Research Foundation (2021A1515110840), Hainan Province Science and Technology Special Fund (ZDYF2021SHFZ250), the Science and Technology Development Fund, Macau SAR (0007/2020/A1, 0020/2022/A1), SKL-QRCM(UM)-2020-2022, QRCM-IRG2022-011, and the University of Macau (MYRG2019-00002-ICMS, MYRG2020-00017-ICMS).

**Data Availability Statement:** Not applicable.

**Conflicts of Interest:** The authors declare no conflict of interest.

## References

1. Thorp, H.H. Proteins, proteins everywhere. *Science* **2021**, *374*, 1415. [CrossRef] [PubMed]
2. Hipp, M.S.; Park, S.H.; Hartl, F.U. Proteostasis impairment in protein-misfolding and -aggregation diseases. *Trends Cell Biol.* **2014**, *24*, 506–514. [CrossRef] [PubMed]
3. Richards, A.L.; Eckhardt, M.; Krogan, N.J. Mass spectrometry-based protein-protein interaction networks for the study of human diseases. *Mol. Syst. Biol.* **2021**, *17*, e8792. [CrossRef] [PubMed]
4. Vilchez, D.; Saez, I.; Dillin, A. The role of protein clearance mechanisms in organismal ageing and age-related diseases. *Nat. Commun.* **2014**, *5*, 5659. [CrossRef] [PubMed]

5. Ma, D.; Tsuboi, T.; Qiu, Y.; Duan, L. Recent progress in ionic iridium(III) complexes for organic electronic devices. *Adv. Mater.* **2017**, *29*, 1603253. [CrossRef]
6. Williams, J.A. The coordination chemistry of dipyridylbenzene: N-deficient terpyridine or panacea for brightly luminescent metal complexes? *Chem. Soc. Rev.* **2009**, *38*, 1783–1801. [CrossRef]
7. Ma, D.-L.; Lin, S.; Wang, W.; Yang, C.; Leung, C.-H. Luminescent chemosensors by using cyclometalated iridium(iii) complexes and their applications. *Chem. Sci.* **2017**, *8*, 878–889. [CrossRef]
8. Ma, D.-L.; Wang, W.; Mao, Z.; Kang, T.-S.; Han, Q.-B.; Chan, P.W.H.; Leung, C.-H. Utilization of G-quadruplex-forming aptamers for the construction of luminescence sensing platforms. *ChemPlusChem* **2017**, *82*, 8–17. [CrossRef]
9. Caporale, C.; Ranieri, A.M.; Paternoster, S.; Bader, C.A.; Falasca, M.; Plush, S.E.; Brooks, D.A.; Stagni, S.; Massi, M. Photophysical and biological properties of iridium tetrazolato complexes functionalised with fatty acid chains. *Inorganics* **2020**, *8*, 23. [CrossRef]
10. Bokareva, O.S.; Möhle, T.; Neubauer, A.; Bokarev, S.I.; Lochbrunner, S.; Kühn, O. Chemical tuning and absorption properties of iridium photosensitizers for photocatalytic applications. *Inorganics* **2017**, *5*, 23. [CrossRef]
11. Chi, Y.; Chou, P.-T. Transition-metal phosphors with cyclometalating ligands: Fundamentals and applications. *Chem. Soc. Rev.* **2010**, *39*, 638–655. [CrossRef]
12. Zhu, X.; Su, Q.; Feng, W.; Li, F. Anti-Stokes shift luminescent materials for bio-applications. *Chem. Soc. Rev.* **2017**, *46*, 1025–1039. [CrossRef]
13. Chelushkin, P.S.; Shakirova, J.R.; Kritchenkov, I.S.; Baigildin, V.A.; Tunik, S.P. Phosphorescent NIR emitters for biomedicine: Applications, advances and challenges. *Dalton Trans.* **2022**, *51*, 1257–1280. [CrossRef]
14. Zhou, J.; Li, J.; Zhang, K.Y.; Liu, S.; Zhao, Q. Phosphorescent iridium(III) complexes as lifetime-based biological sensors for photoluminescence lifetime imaging microscopy. *Coord. Chem. Rev.* **2022**, *453*, 214334. [CrossRef]
15. Wang, W.; Vellaisamy, K.; Li, G.; Wu, C.; Ko, C.-N.; Leung, C.-H.; Ma, D.-L. Development of a long-lived luminescence probe for visualizing β-galactosidase in ovarian carcinoma cells. *Anal. Chem.* **2017**, *89*, 11679–11684. [CrossRef]
16. Wang, W.; Lu, L.; Wu, K.-J.; Liu, J.; Leung, C.-H.; Wong, C.-Y.; Ma, D.-L. Long-lived iridium(III) complexes as luminescent probes for the detection of periodate in living cells. *Sens. Actuators B Chem.* **2019**, *288*, 392–398. [CrossRef]
17. Lo, K.K.-W.; Louie, M.-W.; Zhang, K.Y. Design of luminescent iridium(III) and rhenium(I) polypyridine complexes as in vitro and in vivo ion, molecular and biological probes. *Coord. Chem. Rev.* **2010**, *254*, 2603–2622. [CrossRef]
18. Wu, C.; Wu, K.J.; Liu, J.B.; Zhou, X.M.; Leung, C.H.; Ma, D.L. A dual-functional molecular strategy for in situ suppressing and visualizing of neuraminidase in aqueous solution using iridium(iii) complexes. *Chem. Commun.* **2019**, *55*, 6353–6356. [CrossRef]
19. Wang, W.; Wu, C.; Yang, C.; Li, G.; Han, Q.-B.; Li, S.; Lee, S.M.-Y.; Leung, C.-H.; Ma, D.-L. A dual-functional luminescent probe for imaging $H_2S$ in living zebrafish and discrimination hypoxic cells from normoxic cells. *Sens. Actuators B Chem.* **2018**, *255*, 1953–1959. [CrossRef]
20. Wang, W.; Yung, T.-L.; Cheng, S.-S.; Chen, F.; Liu, J.-B.; Leung, C.-H.; Ma, D.-L. A long-lived luminogenic iridium(III) complex for acetylacetone detection in environmental samples. *Sens. Actuators B Chem.* **2020**, *321*, 128486. [CrossRef]
21. Wang, W.; Dong, Z.-Z.; Yang, C.; Li, G.; Tse, Y.-C.; Leung, C.-H.; Ma, D.-L. An iridium(III) complex-based chemosensor for the detection of thiourea in living cells. *Sens. Actuators B Chem.* **2017**, *251*, 374–379. [CrossRef]
22. Mao, Z.; Liu, J.; Kang, T.-S.; Wang, W.; Han, Q.-B.; Wang, C.-M.; Leung, C.-H.; Ma, D.-L. An Ir(III) complex chemosensor for the detection of thiols. *Sci. Technol. Adv. Mater.* **2016**, *17*, 109–114. [CrossRef] [PubMed]
23. Wang, W.; Mao, Z.; Wang, M.; Liu, L.-J.; Kwong, D.W.J.; Leung, C.-H.; Ma, D.-L. A long lifetime luminescent iridium(iii) complex chemosensor for the selective switch-on detection of $Al^{3+}$ ions. *Chem. Commun.* **2016**, *52*, 3611–3614. [CrossRef] [PubMed]
24. Lo, K.K.-W. Molecular design of bioorthogonal probes and imaging reagents derived from photofunctional transition metal complexes. *Acc. Chem. Res.* **2020**, *53*, 32–44. [CrossRef] [PubMed]
25. Heal, W.P.; Dang, T.H.T.; Tate, E.W. Activity-based probes: Discovering new biology and new drug targets. *Chem. Soc. Rev.* **2011**, *40*, 246–257. [CrossRef]
26. Fang, H.; Peng, B.; Ong, S.Y.; Wu, Q.; Li, L.; Yao, S.Q. Recent advances in activity-based probes (ABPs) and affinity-based probes (AfBPs) for profiling of enzymes. *Chem. Sci.* **2021**, *12*, 8288–8310. [CrossRef]
27. Heinzlmeir, S.; Müller, S. Selectivity aspects of activity-based (chemical) probes. *Drug Discov. Today* **2022**, *27*, 519–528. [CrossRef]
28. Yu, W.; Baskin, J.M. Photoaffinity labeling approaches to elucidate lipid–protein interactions. *Curr. Opin. Chem. Biol.* **2022**, *69*, 102173. [CrossRef]
29. Liu, Y.; Patricelli, M.P.; Cravatt, B.F. Activity-based protein profiling: The serine hydrolases. *Proc. Natl. Acad. Sci. USA.* **1999**, *96*, 14694–14699. [CrossRef]
30. Zuhl, A.M.; Mohr, J.T.; Bachovchin, D.A.; Niessen, S.; Hsu, K.L.; Berlin, J.M.; Dochnahl, M.; Lopez-Alberca, M.P.; Fu, G.C.; Cravatt, B.F. Competitive activity-based protein profiling identifies aza-beta-lactams as a versatile chemotype for serine hydrolase inhibition. *J. Am. Chem. Soc.* **2012**, *134*, 5068–5071. [CrossRef]
31. Wang, Z.; Guo, Z.; Song, T.; Zhang, X.; He, N.; Liu, P.; Wang, P.; Zhang, Z. Proteome-wide identification of on- and off-targets of Bcl-2 inhibitors in native biological systems by using affinity-based probes (AfBPs). *ChemBioChem* **2018**, *19*, 2312–2320. [CrossRef]
32. Yang, X.; Michiels, T.J.M.; de Jong, C.; Soethoudt, M.; Dekker, N.; Gordon, E.; van der Stelt, M.; Heitman, L.H.; van der Es, D.; AP, I.J. An affinity-based probe for the human adenosine A2A receptor. *J. Med. Chem.* **2018**, *61*, 7892–7901. [CrossRef]
33. Sheinenzon, A.; Shehadeh, M.; Michelis, R.; Shaoul, E.; Ronen, O. Serum albumin levels and inflammation. *Int. J. Biol. Macromol.* **2021**, *184*, 857–862. [CrossRef] [PubMed]

34. Zhao, Y.; Li, J.; Wu, Z.; Zhang, H.; Zhao, Y.; Yang, R.; Lu, L. Curcumin ligand based iridium(III) complexes as inhibition and visualization agent of beta-amyloid fibrillation. *Microchem. J.* **2021**, *160*, 105721. [CrossRef]
35. Srivastava, S.; Koay, E.J.; Borowsky, A.D.; De Marzo, A.M.; Ghosh, S.; Wagner, P.D.; Kramer, B.S. Cancer overdiagnosis: A biological challenge and clinical dilemma. *Nat. Rev. Cancer* **2019**, *19*, 349–358. [CrossRef]
36. Bray, F.; Ferlay, J.; Soerjomataram, I.; Siegel, R.L.; Torre, L.A.; Jemal, A. Global cancer statistics 2018: Globocan estimates of incidence and mortality worldwide for 36 cancers in 185 countries. *CA Cancer J. Clin.* **2018**, *68*, 394–424. [CrossRef]
37. Bogani, G.; Ditto, A.; Raspagliesi, F. Early diagnosis in endometrial cancer minimizes the impact of treatments. *Am. J. Obstet. Gynecol.* **2018**, *219*, 631–632. [CrossRef]
38. Whitaker, K. Earlier diagnosis: The importance of cancer symptoms. *Lancet Oncol.* **2020**, *21*, 6–8. [CrossRef]
39. Lo, K.K.-W.; Zhang, K.Y.; Chung, C.-K.; Kwok, K.Y. Synthesis, photophysical and electrochemical properties, and protein-binding studies of luminescent cyclometalated iridium(III) bipyridine estradiol conjugates. *Chem. Eur. J.* **2007**, *13*, 7110–7120. [CrossRef]
40. Sun, T.; Liu, Z.; Yang, Q. The role of ubiquitination and deubiquitination in cancer metabolism. *Mol. Cancer* **2020**, *19*, 146. [CrossRef]
41. Caon, I.; Bartolini, B.; Parnigoni, A.; Carava, E.; Moretto, P.; Viola, M.; Karousou, E.; Vigetti, D.; Passi, A. Revisiting the hallmarks of cancer: The role of hyaluronan. *Semin. Cancer Biol.* **2020**, *62*, 9–19. [CrossRef]
42. Smith, W.L.; Langenbach, R. Why there are two cyclooxygenase isozymes. *J. Clin. Investig.* **2001**, *107*, 1491–1495. [CrossRef] [PubMed]
43. Uchida, K. HNE as an inducer of COX-2. *Free Radic. Biol. Med.* **2017**, *111*, 169–172. [CrossRef] [PubMed]
44. Uddin, M.J.; Crews, B.C.; Xu, S.; Ghebreselasie, K.; Daniel, C.K.; Kingsley, P.J.; Banerjee, S.; Marnett, L.J. Antitumor activity of cytotoxic cyclooxygenase-2 Inhibitors. *ACS Chem. Biol.* **2016**, *11*, 3052–3060. [CrossRef] [PubMed]
45. Liu, C.; Yang, C.; Lu, L.; Wang, W.; Tan, W.; Leung, C.H.; Ma, D.L. Luminescent iridium(iii) complexes as COX-2-specific imaging agents in cancer cells. *Chem. Commun.* **2017**, *53*, 2822–2825. [CrossRef]
46. Slack, R.J.; Macdonald, S.J.F.; Roper, J.A.; Jenkins, R.G.; Hatley, R.J.D. Emerging therapeutic opportunities for integrin inhibitors. *Nat. Rev. Drug Discov.* **2022**, *21*, 60–78. [CrossRef]
47. Ma, X.; Jia, J.; Cao, R.; Wang, X.; Fei, H. Histidine-iridium(III) coordination-based peptide luminogenic cyclization and cyclo-RGD peptides for cancer-cell targeting. *J. Am. Chem. Soc.* **2014**, *136*, 17734–17737. [CrossRef]
48. Cancilla, D.; Rettig, M.P.; DiPersio, J.F. Targeting CXCR4 in AML and ALL. *Front. Oncol.* **2020**, *10*, 1672. [CrossRef]
49. Bhandari, D.; Robia, S.L.; Marchese, A. The E3 ubiquitin ligase atrophin interacting protein 4 binds directly to the chemokine receptor CXCR4 via a novel WW domain-mediated interaction. *Mol. Biol. Cell* **2009**, *20*, 1324–1339. [CrossRef]
50. Furusato, B.; Mohamed, A.; Uhlen, M.; Rhim, J.S. CXCR4 and cancer. *Pathol. Int.* **2010**, *60*, 497–505. [CrossRef]
51. Kang, H.; Watkins, G.; Douglas-Jones, A.; Mansel, R.E.; Jiang, W.G. The elevated level of CXCR4 is correlated with nodal metastasis of human breast cancer. *Breast* **2005**, *14*, 360–367. [CrossRef]
52. Kuil, J.; Steunenberg, P.; Chin, P.T.; Oldenburg, J.; Jalink, K.; Velders, A.H.; van Leeuwen, F.W. Peptide-functionalized luminescent iridium complexes for lifetime imaging of CXCR4 expression. *ChemBioChem* **2011**, *12*, 1897–1903. [CrossRef]
53. Nayak, R.T.; Hong, H.; Zhang, Y.; Cai, W. Multimodality imaging of CXCR4 in cancer: Current status towards clinical translation. *Curr. Mol. Med.* **2013**, *13*, 1538–1548. [CrossRef]
54. Chen, J.; Zeng, F.; Forrester, S.J.; Eguchi, S.; Zhang, M.Z.; Harris, R.C. Expression and function of the epidermal growth factor receptor in physiology and disease. *Plant Physiol.* **2016**, *96*, 1025–1069. [CrossRef]
55. Li, Z.; Tyrpak, D.R.; Park, M.; Okamoto, C.T.; MacKay, J.A. A new temperature-dependent strategy to modulate the epidermal growth factor receptor. *Biomaterials* **2018**, *183*, 319–330. [CrossRef]
56. Gazit, A.; Yaish, P.; Gilon, C.; Levitzki, A. Tyrphostins I: Synthesis and biological activity of protein tyrosine kinase inhibitors. *J. Med. Chem.* **1989**, *32*, 2344–2352. [CrossRef] [PubMed]
57. Wu, C.; Wu, K.-J.; Liu, J.-B.; Wang, W.; Leung, C.-H.; Ma, D.-L. Structure-guided discovery of a luminescent theranostic toolkit for living cancer cells and the imaging behavior effect. *Chem. Sci.* **2020**, *11*, 11404–11412. [CrossRef]
58. Baratto, L.; Duan, H.; Macke, H.; Iagaru, A. Imaging the distribution of gastrin-releasing peptide receptors in cancer. *J. Nucl. Med.* **2020**, *61*, 792–798. [CrossRef]
59. Constantinides, C.; Lazaris, A.C.; Haritopoulos, K.N.; Pantazopoulos, D.; Chrisofos, M.; Giannopoulos, A. Immunohistochemical detection of gastrin releasing peptide in patients with prostate cancer. *World J. Urol.* **2003**, *21*, 183–187. [CrossRef]
60. Sano, H.; Feighner, S.D.; Hreniuk, D.L.; Iwaasa, H.; Sailer, A.W.; Pan, J.; Reitman, M.L.; Kanatani, A.; Howard, A.D.; Tan, C.P. Characterization of the bombesin-like peptide receptor family in primates. *Genomics* **2004**, *84*, 139–346. [CrossRef]
61. Wang, W.; Wu, K.J.; Vellaisamy, K.; Leung, C.H.; Ma, D.L. Peptide-conjugated long-lived theranostic imaging for targeting GRPr in cancer and immune cells. *Angew. Chem. Int. Ed.* **2020**, *59*, 17897–17902. [CrossRef] [PubMed]
62. Sobczuk, P.; Lomiak, M.; Cudnoch-Jedrzejewska, A. Dopamine D1 receptor in cancer. *Cancers* **2020**, *12*, 3232. [CrossRef] [PubMed]
63. Prabhu, V.V.; Madhukar, N.S.; Gilvary, C.; Kline, C.L.B.; Oster, S.; El-Deiry, W.S.; Elemento, O.; Doherty, F.; VanEngelenburg, A.; Durrant, J.; et al. Dopamine receptor D5 is a modulator of tumor response to dopamine receptor D2 antagonism. *Clin. Cancer Res.* **2019**, *25*, 2305–2313. [CrossRef] [PubMed]
64. Butini, S.; Nikolic, K.; Kassel, S.; Bruckmann, H.; Filipic, S.; Agbaba, D.; Gemma, S.; Brogi, S.; Brindisi, M.; Campiani, G.; et al. Polypharmacology of dopamine receptor ligands. *Prog. Neurobiol.* **2016**, *142*, 68–103. [CrossRef] [PubMed]

65. Vellaisamy, K.; Li, G.; Ko, C.N.; Zhong, H.J.; Fatima, S.; Kwan, H.Y.; Wong, C.Y.; Kwong, W.J.; Tan, W.; Leung, C.H.; et al. Cell imaging of dopamine receptor using agonist labeling iridium(iii) complex. *Chem. Sci.* **2018**, *9*, 1119–1125. [CrossRef]
66. Burke, P.J. Mitochondria, bioenergetics and apoptosis in cancer. *Trends Cancer* **2017**, *3*, 857–870. [CrossRef]
67. Nagata, S. Apoptosis and clearance of apoptotic cells. *Annu. Rev. Immunol.* **2018**, *36*, 489–517. [CrossRef]
68. Tang, D.; Lotze, M.T.; Kang, R.; Zeh, H.J. Apoptosis promotes early tumorigenesis. *Oncogene* **2011**, *30*, 1851–1854. [CrossRef]
69. Vunnam, N.; Szymonski, S.; Hirsova, P.; Gores, G.J.; Sachs, J.N.; Hackel, B.J. Noncompetitive allosteric antagonism of death receptor 5 by a synthetic affibody ligand. *Biochemistry* **2020**, *59*, 3856–3868. [CrossRef]
70. Zhang, B.; van Roosmalen, I.A.M.; Reis, C.R.; Setroikromo, R.; Quax, W.J. Death receptor 5 is activated by fucosylation in colon cancer cells. *FEBS J.* **2019**, *286*, 555–571. [CrossRef]
71. Masum, A.A.; Yokoi, K.; Hisamatsu, Y.; Naito, K.; Shashni, B.; Aoki, S. Design and synthesis of a luminescent iridium complex-peptide hybrid (IPH) that detects cancer cells and induces their apoptosis. *Bioorg. Med. Chem.* **2018**, *26*, 4804–4816. [CrossRef]
72. Lesch, H.P.; Kaikkonen, M.U.; Pikkarainen, J.T.; Ylä-Herttuala, S. Avidin-biotin technology in targeted therapy. *Expert Opin. Drug Deliv.* **2010**, *7*, 551–564. [CrossRef]
73. Luong, J.H.T.; Male, K.B.; Glennon, J.D. Biotin interference in immunoassays based on biotin-strept(avidin) chemistry: An emerging threat. *Biotechnol. Adv.* **2019**, *37*, 634–641. [CrossRef]
74. Lo, K.K.-W.; Chan, J.S.-W.; Lui, L.-H.; Chung, C.-K. Novel luminescent cyclometalated iridium(III) diimine complexes that contain a biotin moiety. *Organometallics* **2004**, *23*, 3108–3116. [CrossRef]
75. Lo, K.K.-W.; Li, C.-K.; Lau, J.S.-Y. Luminescent cyclometalated iridium(III) arylbenzothiazole biotin complexes. *Organometallics* **2005**, *24*, 4594–4601. [CrossRef]
76. Lo, K.K.-W.; Chung, C.-K.; Zhu, N. Nucleic acid intercalators and avidin probes derived from luminescent cyclometalated iridium(III)–dipyridoquinoxaline and –dipyridophenazine complexes. *Chem. Eur. J.* **2006**, *12*, 1500–1512. [CrossRef]
77. Lo, K.K.-W.; Lau, J.S.-Y. Cyclometalated iridium(III) diimine bis(biotin) complexes as the first luminescent biotin-based cross-linkers for avidin. *Inorg. Chem.* **2007**, *46*, 700–709. [CrossRef]
78. Zhang, K.Y.; Lo, K.K.-W. Synthesis, properties, and live-cell imaging studies of luminescent cyclometalated iridium(III) polypyridine complexes containing two or three biotin pendants. *Inorg. Chem.* **2009**, *48*, 6011–6025. [CrossRef]
79. Zhang, K.Y.; Liu, H.-W.; Tang, M.-C.; Choi, A.W.-T.; Zhu, N.; Wei, X.-G.; Lau, K.-C.; Lo, K.K.-W. Dual-emissive cyclometalated iridium(III) polypyridine complexes as ratiometric biological probes and organelle-selective bioimaging reagents. *Inorg. Chem.* **2015**, *54*, 6582–6593. [CrossRef]
80. Kwon, T.-H.; Kwon, J.; Hong, J.-I. Signal amplification via intramolecular energy transfer using tripodal neutral iridium(III) complexes upon binding to avidin. *J. Am. Chem. Soc.* **2008**, *130*, 3726–3727. [CrossRef]
81. Raabe, C.A.; Groper, J.; Rescher, U. Biased perspectives on formyl peptide receptors. *BBA-Mol. Cell Res.* **2019**, *1866*, 305–316. [CrossRef] [PubMed]
82. Li, Z.; Li, Y.; Han, J.; Zhu, Z.; Li, M.; Liu, Q.; Wang, Y.; Shi, F.-D. Formyl peptide receptor 1 signaling potentiates inflammatory brain injury. *Sci. Transl. Med.* **2021**, *13*, eabe9890. [CrossRef] [PubMed]
83. Vellaisamy, K.; Li, G.; Wang, W.; Leung, C.H.; Ma, D.L. A long-lived peptide-conjugated iridium(iii) complex as a luminescent probe and inhibitor of the cell migration mediator, formyl peptide receptor 2. *Chem. Sci.* **2018**, *9*, 8171–8177. [CrossRef] [PubMed]
84. Ma, H.; Guo, X.; Wang, Z.; Han, M.; Liu, H. Therapeutic potential of WKYMVm in diseases. *Front. Pharmacol.* **2022**, *13*, 986963. [CrossRef]
85. Liu, T.; Zhang, L.; Joo, D.; Sun, S.C. NF-kappaB signaling in inflammation. *Signal Transduct. Target. Ther.* **2017**, *2*, 17023. [CrossRef]
86. Imbert, V.; Peyron, J.F. NF-kappaB in hematological malignancies. *Biomedicines* **2017**, *5*, 27. [CrossRef]
87. Wang, W.; Yang, C.; Lin, S.; Vellaisamy, K.; Li, G.; Tan, W.; Leung, C.H.; Ma, D.L. First synthesis of an oridonin-conjugated iridium(III) complex for the intracellular tracking of NF-kappaB in living cells. *Chem. Eur. J.* **2017**, *23*, 4929–4935. [CrossRef]
88. China, L.; Skene, S.S.; Shabir, Z.; Maini, A.; Sylvestre, Y.; Bennett, K.; Bevan, S.; O'Beirne, J.; Forrest, E.; Portal, J.; et al. Administration of albumin solution increases serum levels of albumin in patients with chronic liver failure in a single-arm feasibility trial. *Clin. Gastroenterol. Hepatol.* **2018**, *16*, 748–755.e6. [CrossRef]
89. Wang, Y.; Huang, H.; Chen, G.; Chen, H.; Xu, T.; Tang, Q.; Zhu, H.; Zhang, Q.; Zhang, P. A novel iridium(iii) complex for sensitive HSA phosphorescence staining in proteome research. *Chem. Commun.* **2018**, *54*, 3282–3285. [CrossRef]
90. Panza, F.; Lozupone, M.; Logroscino, G.; Imbimbo, B.P. A critical appraisal of amyloid-β-targeting therapies for Alzheimer disease. *Nat. Rev. Neurol.* **2019**, *15*, 73–88. [CrossRef]
91. Han, J.; Du, Z.; Lim, M.H. Mechanistic insight into the design of chemical tools to control multiple pathogenic features in Alzheimer's disease. *Acc. Chem. Res.* **2021**, *54*, 3930–3940. [CrossRef]
92. Fusar-Poli, L.; Vozza, L.; Gabbiadini, A.; Vanella, A.; Concas, I.; Tinacci, S.; Petralia, A.; Signorelli, M.S.; Aguglia, E. Curcumin for depression: A meta-analysis. *Crit. Rev. Food Sci. Nutr.* **2020**, *60*, 2643–2653. [CrossRef]
93. Banik, U.; Parasuraman, S.; Adhikary, A.K.; Othman, N.H. Curcumin: The spicy modulator of breast carcinogenesis. *J. Exp. Clin. Canc. Res.* **2017**, *36*, 98. [CrossRef]
94. McGhie, B.S.; Aldrich-Wright, J.R. Photoactive and luminescent transition metal complexes as anticancer agents: A guiding light in the search for new and improved cancer treatments. *Biomedicines* **2022**, *10*, 578. [CrossRef]

95. Ma, D.-L.; Wu, C.; Cheng, S.-S.; Lee, F.-W.; Han, Q.-B.; Leung, C.-H. Development of natural product-conjugated metal complexes as cancer therapies. *Int. J. Mol. Sci.* **2019**, *20*, 341. [CrossRef]
96. Poursharifi, M.; Wlodarczyk, M.T.; Mieszawska, A.J. Nano-based systems and biomacromolecules as carriers for metallodrugs in anticancer therapy. *Inorganics* **2019**, *7*, 2. [CrossRef]